Review

Genetically Encoded Calcium Indicators

Marco Mank, and Oliver Griesbeck

Chem. Rev., **2008**, 108 (5), 1550-1564 • DOI: 10.1021/cr078213v • Publication Date (Web): 01 May 2008

Genetically Encoded Calcium Indicators

Marco Mank and Oliver Griesbeck*

Max-Planck-Institut für Neurobiologie, Am Klopferspitz 18, 82152 Martinsried, Germany

Received November 9, 2007

Contents

1. Introduction 1550
2. Calcium Binding Protein Motifs 1551
3. Genetically Encoded Calcium Indicators 1553
   3.1. FRET-Based Sensors Employing Calmodulin (CaM) 1553
   3.2. FRET-Based Sensors Employing Troponin C (TnC) 1555
   3.3. Single Fluorophore Sensors 1556
4. *In Vitro* Kinetics 1558
5. *In Vitro* versus *in Vivo* Performance 1560
6. Detecting Neuronal Activity 1562
7. Conclusions 1563
8. Acknowledgments 1563
9. References 1563

1. Introduction

One of the greatest challenges in neuroscience has been to monitor electrical activity and biochemistry in populations of identified neurons *in vivo*.[1] Recent work on new microscopy techniques has moved the field considerably further in that direction. In particular the combination of modern imaging technology and genetic labeling methods heralds a bright future for neuronal circuit analysis.[2–5] Biosensor development complements these efforts on the "indicator side" by providing probes for key events crucial for an understanding of neuronal function and plasticity. Moreover it aims at overcoming long-standing limitations in the ability to monitor neuronal activity and biochemistry in intact tissues and over longer periods of time.

The term "genetically encoded" refers to the fact that the sensors are solely composed of amino acids with no addition of any synthetic compound or cofactor that would be difficult to apply into a living brain. Thus, sensors are encoded by a stretch of DNA that can be manipulated, mutated, and concatenated by any technique that the recombinant DNA toolbox offers. When DNA coding for the sensor is delivered into a cell, the sensor is formed within the cell *in situ*. Combined with the use of cell-type specific promoters, cellular targeting sequences, and transgenic technology, this offers a noninvasive means to implant an indicator deeply within a tissue of a living organism with cellular and subcellular specificity.

Genetically encoded indicators use the Green Fluorescent Protein (GFP) or more generally speaking autofluorescent proteins (XFPs) and mutants thereof as fluorophores with all the advantages and restrictions that these fascinating proteins possess.[6–9] Currently the XFPs are the only known family of proteins that form an internal fluorophore in aerobic environments via an autocatalytic reaction involving a number of critical amino acid residues within the peptide backbone.[10,11] Therefore progress on the biosensor side is closely linked with further improvements in engineering XFPs for more brightness, photostability, full maturation at 37 °C, and shifts to longer wavelengths of emission.

In its strictest sense the term "genetically encoded calcium indicators" (GECIs) also includes other types of sensors that operate with chemiluminescence, such as aequorin and derived sensors that use chemiluminescence energy transfer from aequorin to GFP.[12–15] While offering some advantages compared to fluorescent reporters such as lack of background fluorescence and the ease of working with freely moving animals, the difficulty of obtaining high spatial resolution makes these sensors less suitable for many brain imaging applications. As the topic is relatively large, these probes will not be covered here in more detail. Instead the reader is invited to consult other reviews.[12,16–18]

Traditionally optical measurements of free cytosolic calcium fluctuations have been perfomed using a collection of synthetic organic molecules that change fluorescence or absorbance properties upon calcium binding. The field was revolutionized by the work of Roger Y. Tsien, who generated a series of fluorescent polycarboxylate compounds with strongly improved fluorescence properties. Both single-wavelength indicators and indicators suitable for ratiometric imaging were established. Tsien also introduced noninvasive methods of loading the compounds into living cells as acetoxymethyl esters.[19,20] During the last two decades improvements in design and performance were incorporated. Currently, the best dyes are characterized by large fractional fluorescence changes (for example an approximately 14-fold relative intensity change for the indicator Oregon Green BAPTA-1; www.invitrogen.com), very good selectivity for calcium versus other cations, fast binding and dissociation kinetics, fairly linear response properties, pH-resistance, and photostability. Thus, synthetic fluorescent calcium probes provide a standard of performance parameters that genetically encoded calcium indicators will be compared with.

Measurements of free cellular calcium have received special interest in the neurosciences, because the geometry and high degree of compartmentalization of neurons, together with an exquisite collection of calcium channels specific to neurons, has added another twist to the already ravishing complexity of cellular calcium handling and signaling. Moreover, rises in cytosolic calcium can be used as a relatively direct measure of neuronal activity. When a neuron fires action potentials, voltage-gated calcium channels in the plasma membrane open up and lead to a rise in cytosolic calcium within a few milliseconds. Due to the relatively large

* To whom correspondence should be addressed. E-mail: griesbeck@neuro.mpg.de.

10.1021/cr078213v CCC: $71.00
Published on Web 05/01/2008

Marco Mank studied biology at the University of Würzburg. Since 2004, he has been working toward a Ph.D. at the Max-Planck-Institute of Neurobiology, Martinsried.

Dr. Oliver Griesbeck studied biology and obtained a Ph.D. in Neuroscience from the University of Munich in 1997. He then worked as research associate of the Howard Hughes Medical Institute at the University of California, San Diego. At the end of 2001, he accepted a position at the Max-Planck-Institute of Neurobiology in Martinsried, Germany, where he is currently the leader of a Junior Research Group.

fractional fluorescence changes of synthetic calcium indicators, they have been preferably used to monitor activity of large numbers of neurons optically within tissue slices or within the brain of living animals *in vivo*.[21,22] Unfortunately, there exist a number of disadvantages that complicate the use of synthetic calcium dyes in intact neuronal tissue. It is often hard to achieve satisfactory loading of neuronal tissue using acetoxymethyl esters of synthetic probes, especially when the tissue is more mature or encapsulated in connective tissue such as some peripheral ganglia. Dye loading does not work in cells with thick cell walls and small model organisms with strong body walls and cuticulae such as the nematode *Caenorhabditis elegans* or the fruit fly *Drosophila melanogaster*. The dyes can compartmentalize in an uncontrolled manner to cellular organelles or leak out of the cells during longer recording periods, making chronic imaging of neurons as they undergo structural plasticity or regeneration impossible. The dye loading does not allow any cell type specificity, but labels tissue indiscriminately. Labeling of neuronal architecture is often diffuse and does not reveal processes in a satisfactory manner when ester loading is used. No subcellular labeling specificity such as labeling of individual pre- or postsynaptic sites is possible. Therefore the ability to target fluorescent sensors with the means of molecular biology is desirable Although genetic targeting of synthetic indicators appears feasible, it has so far only been demonstrated in cultured cells *in vitro*.[23]

While calcium imaging for practical reasons is currently the preferred optical read-out modus for neuronal activity *in vivo*, changes in membrane potential are the most direct way to study neuronal activity. Accordingly, a number of genetically encoded voltage sensors have also been developed, which may still lack performance for *in vivo* work but should be considered as serious platforms for further improvements.[24–26] In this article we will review the current state of the art of genetically encoded calcium indicators, outline the basic design principles and engineering strategies, pinpoint the strengths and weaknesses that the existing indicators have, and discuss goals and milestones for indicator performance that would be desirable to reach in the future.

2. Calcium Binding Protein Motifs

Protein-based calcium chelation is the initial step in the cascade leading to manipulation of a biosensor's fluorescence output. The nature of these binding sites determines the properties of a biosensor and the design options for sensor construction. It is therefore worthwhile to have a closer look at the molecular constitution and functional characteristics of these motifs.

Apart from some unconventional calcium-binding sites (for example in calpains or the Na^+/Ca^{2+} exchanger) there are two prominent types of intracellular calcium-binding motifs that can coordinate calcium in the physiologically relevant range.[27,28] These motifs are the C2 domain and the EF-hand. The C2 domain is found in a huge variety of different proteins, e.g., PLA_2 (phospholipase A2), PLC (phospholipase C), PKC (protein kinase C), and synaptotagmin.[29] A feature of many C2 domains is that they bind calcium and phospholipids, although there are variants that have evolved to bind other targets. PKC was the first protein where the C2 domain was found. It consists of ~130 amino acid residues, and the structure reveals a scaffold consisting of eight β-sheets (Figure 1A). On top of this scaffold three loops are attached that promote calcium and phospholipid binding. It is interesting to note that the coordination sphere is provided by residues that are not neighbored in the linear sequence and that the phospholipid can act as a ligand for calcium binding, as has been shown for the PKC-C2 domain (Figure 1C).[30] Calcium can be bound in the absence of a phospholipid, although the presence of the latter increases the affinity for calcium. For example the K_d value for calcium of the C_2A domain of synaptotagmin I is >1 mM but can be decreased about 1000-fold in the presence of phospholipids.[29] Upon calcium binding, C2 domains apparently do not display a significant structural rearrangement of the protein backbone, as was shown for the C_2A domain of synaptotagmin I.[31] Due to the interrelationship between phospholipid and calcium binding, the large domain size with chelating residues distributed far apart and the possible binding to other target C2 domains are not a first choice for indicator construction.

Thus a more suitable candidate for GECIs is the famous calcium-binding protein domain called EF-hand. It was first described in parvalbumin and represents a helix–loop–helix motif of ~30 amino acids that is capable of coordinating one calcium (or magnesium) ion.[32] Usually EF-hands occur as pairs in proteins so that most EF-hand-containing polypeptides have two, four, six, or more EF-hand domains (Figure 1B). The most important part of the domain is the loop

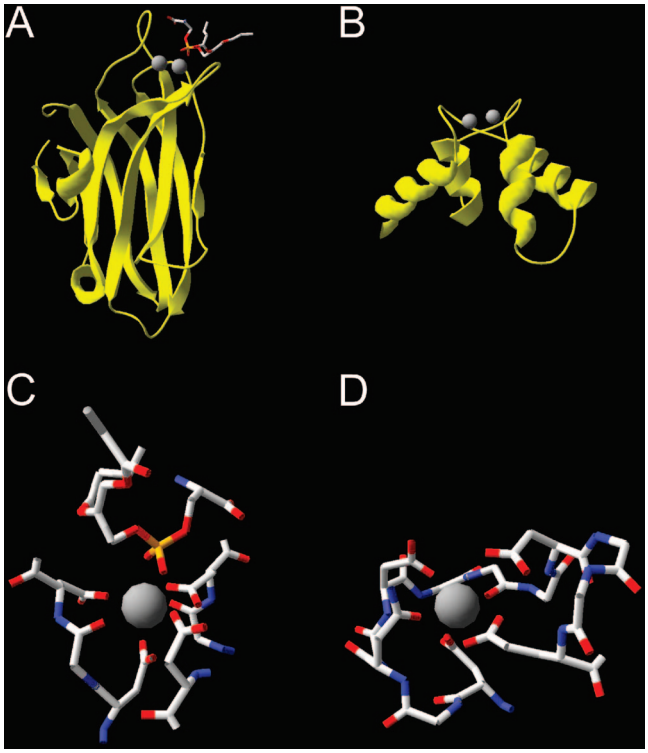

Figure 1. Comparison of two intracellular Ca^{2+}-binding domains C2 and EF-hand. (A) Structure of the C2 domain of PKCα (pdb file 1DSY) complexed with calcium and 1,2-dicaproyl-*sn*-phosphatidyl-L-serine. (B) C-terminal EF-hand domain of chicken skeletal troponin C (csTnC, pdb file 1TOP) complexed with calcium. (C) Blowup of the Ca^{2+} (1) coordination in PKCα-C2. (D) Blowup of the coordination in EF-hand III of csTnC. All structures were redrawn using DeepView/Swiss-PdbViewer 3.7.

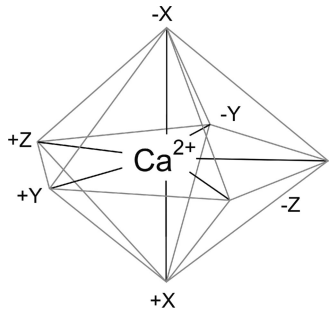

Figure 2. Schematic of the calcium coordination in a canonical EF-hand. Depicted are positions of the residues that are involved in the calcium coordination. Note that two ligands in the planar pentagon are provided by the same amino acid residue (−Z).

region, which gives rise to the coordination space through predominantly negatively charged amino acid residues (Figure 1D). Most EF-hand-containing proteins possess the so-called canonical EF-hand. This version of the domain exhibits a 12-residue calcium-binding loop consisting of nine residues in the loop region and three residues in the exiting helical part of the EF-hand (Figure 2). The canonical EF-hand coordinates the calcium ion via a pentagonal bipyramid, i.e., through seven coordinating partners. The positions inside the 12-residue binding loop are referred to as

$$1(+X),\ 3(+Y),\ 5(+Z),\ 7(-Y),\ 1(-X),\ 12(-Z),$$

Numbers indicate the position along the linear sequence of the loop, whereas letters indicate the position in the 3D geometry of the pentagonal bipyramid (Figure 2). Amino acid residues in the Y and Z positions belong to the planar pentagon with a glutamic acid at −Z that provides two chelating groups as a bidentate side chain. The X positions complete the coordination space for calcium and correspond to the tips of the bipyramid.[33] Although most chelating groups arise from the amino acid residues, there is one exception found in the canonical EF-hand. This exclusion is displayed by position 7(−Y), which coordinates the calcium ion with its carbonyl group of the peptide backbone. Additionally the amino acid residue at position 9(−X) is able to coordinate the ion either directly or through a bridged water molecule. A hydrophobic amino acid residue at position 8 (Ile, Val, or Leu) plays another important role: as mentioned before, EF-hands are usually found as pairs in EF-hand-containing peptides. The residue stabilizes the paired EF-hand domain via a short β-sheet with the corresponding hydrophobic residue in the second EF-hand.[34]

In contrast to the C2 domain many EF-hands display a structural rearrangement, elicited by the calcium coordination. The EF-hand pair undergoes a transition of almost parallel helices of one EF-hand in the apo (unbound or closed) state to perpendicular helices in the bound (open) state. In case of calmodulin this conformational change exposes a hydrophobic surface that is the basis of target recognition.[33]

Some of the EF-hands are able to bind not only calcium but also magnesium. They are referred to as Ca^{2+}/Mg^{2+} EF-hands. Two crucial features can be observed in such EF domains, namely, a Z-acid pair or an aspartic acid in position 12.[33,35] The coordination space for the magnesium ion exhibits an octahedral geometry; thus in some of the Ca^{2+}/Mg^{2+} EF-hands the bidentate amino acid residue at position 12 coordinates the ion through one of its oxygens, while calcium binding is promoted with both oxygens of the side chain. In EF-hands III and IV of troponin C magnesium binding can induce a structural change and interferes with calcium binding.[36,37]

According to their effector function essentially two categories of EF-hands can be discriminated: "regulatory" EF-hands that undergo a conformational change after calcium binding and "structural" EF-hands that do not.[34] The regulatory hands are typical of proteins with important regulatory function such as calmodulin, troponin C, and recoverin. These proteins typically mediate effects of calcium on physiology and biochemistry of a cell. The structural EF-hands occur in buffer proteins such as calbindin D9K or parvalbumin and serve to shape the profile and duration of calcium signals within cells.

Typically EF-hands occur as pairs in proteins that are stacked against each other and provide mutual stabilization. As a consequence, calcium binding to EF-hands is usually cooperative. In general positive cooperativity is observed because calcium binding to an EF-hand has positive structural effects on the "partner" hand, facilitating calcium binding to this hand. A certain challenge therefore may lie in tuning such a sensor mechanism to obtain linear reporters of calcium and neuronal activity. Due to the paired functional EF-hand module, EF-hand-containing polypeptides are often built in a modular fashion and have two, four, six, or more EF-hand domains.[38] Some of the smaller calcium-binding proteins such as troponin C and calmodulin are constituted almost exclusively of 4 EF-hand motifs (Figure 3). Each pair of hands in these proteins forms a globular lobe domain named the N-terminal and C-terminal lobe. The domains are structurally independent and differ considerably in terms of calcium-binding properties and biological function.[36,39] The

```
MASMTDQQAEARAFLSEEMIAEFKAAFDMFDADG-GGDISTKELGTVMRMLGQNPTK
---MDDIYKAAVEQLTEEQKNEFKAAFDIFVLGAEDGCISTKELGKVMRMLGQNPTP
---MA-------DQLTEEQIAEFKEAFSLFDKDG-DGTITTKELGTVMRSLGQNPTE

EELDAIIEEVDEDGSGTIDFEEFLVMMVRQMKEDAKGKSEEELANCFRIFDKNADGF
EELQEMIDEVDEDGSGTVDFDEFLVMMVRCMKDDSKGK-SEELSDLFRMFDKNADGY
AELQDMINEVDADGNGTIDFPEFLTMMARKMKDT---DSEEEIREAFRVFDKDGNGY

IDIEELGEILRATGEHVIEEDIEDLMKDSDKNNDGRIDFDEFLKMMEGVQ  csTnC
IDLDELKIMLQATGETITEDDIEELMKDGDKNNDGRIDYDEFLEFMKGVE  hcTnC
ISAAELRHVMTNLGEKLTDEEVDEMIREADIDGDGQVNYEEFVQMMTA-K  XCaM
```

Figure 3. Alignment of chicken skeletal troponin C (csTnC), human cardiac troponin C (hcTnC), and *Xenopus* calmodulin (XCaM). Calcium-binding loops of functional EF-hands are colored according to their position inside the protein. In case of hcTnC the first EF-hand is not functional.

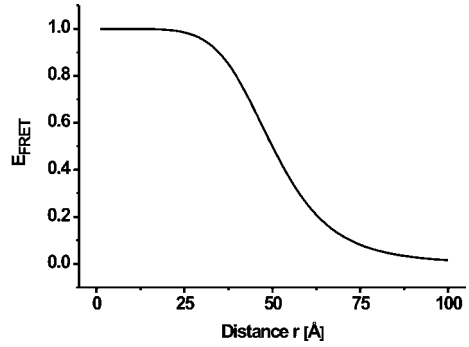

Figure 4. Dependency of FRET efficiency (E_{FRET}) on the distance (r) between a donor/acceptor pair with an assumed Förster radius R_0 of 50 Å. Note that the relationship is only linear with distance changes in the vicinity of R_0. Therefore an idealized, approximately linear FRET reporter will preferably operate at E_{FRET} values between 0.2 and 0.8.

different nature of these domains should be kept in mind when using such a protein as binding domain within a biosensor.

3. Genetically Encoded Calcium Indicators

The fluorescence of known XFPs in their native forms is in general insensitive to changes in calcium concentration, although a number of other environmental sensitivities exist such as sensitivities to pH fluctuations or halides in yellow fluorescent protein variants.[40–42] These endogenous sensitivities can be exploited for use as physiological sensors of pH or chloride or further enhanced by mutagenesis of the protein variant.[43,44] To confer calcium sensitivity to an XFP, the calcium-binding abilities of other proteins, as discussed in the previous section, have to be recruited. Calcium biosensors are therefore based on XFPs and a calcium-binding protein moiety that have to be fused to each other in such a way that calcium binding maximally modulates fluorescence properties of such a chimeric construct. There are essentially two paradigms of constructing genetically encoded calcium indicators that will be discussed separately. One employs FRET (Förster resonance energy transfer) between two suitable mutants of XFPs. A second approach is based on calcium-mediated modulation of the fluorescence properties of a single XFP as fluorophore.

3.1. FRET-Based Sensors Employing Calmodulin (CaM)

Förster (or often fluorescence) resonance energy transfer is a spectroscopic phenomenon sensitive to changes in conformation, orientation, and distance of two fluorophores in dimensions below 100 Å.[45,46] The excited-state energy of an excited donor is hereby transferred to an acceptor fluorophore, and efficiency of this transfer is quantitatively described by the Förster equation. FRET efficiency steeply falls off with increasing distance between the fluorophores following (Figure 4)

$$E_{FRET} = \frac{R_0^6}{R_0^6 + r^6} \quad (1)$$

In this term r is the actual distance between the fluorophores and R_0 is the distance (also called Förster distance) at which energy transfer between a given donor–acceptor pair is half-maximal. It should be noted that R_0 is a specific value for each individual donor–acceptor pair that depends on spectral overlap between donor emission and acceptor excitation, the donor quantum yield, and an orientation factor κ^2. Typically, Förster distances are in the range 20–80 Å. The suitability of spectral mutants of GFPs for FRET had been recognized early.[47] The dependence of FRET on distance and orientation has subsequently been exploited for the generation of two pioneering prototypical FRET biosensors.

In one example, a calmodulin-binding peptide from smooth muscle myosin light chain kinase (smMLCK) was sandwiched between a Blue Fluorescent Protein (BFP) and a Green Fluorescent Protein (Figure 5).[48] Strictly speaking, the resulting indicator named FIP-CB_{SM} was not a calcium biosensor per se, but reported binding of Ca^{2+}/calmodulin to its binding peptide, upon which FRET from BFP to GFP was disrupted. The effect of calmodulin binding to its peptide was quantified by acquiring ratios of acceptor and donor emission intensities. Due to its mode of action, any estimates on free calcium were only indirect and showed moderate kinetics. For studies in live cells the sensor was microinjected in HEK 293 cells. Free recombinant calmodulin was however co-injected, as the availability of endogenous calmodulin turned out to be limiting for sensor function.

In another approach calmodulin and its binding peptide M13 from myosin light chain kinase were sandwiched

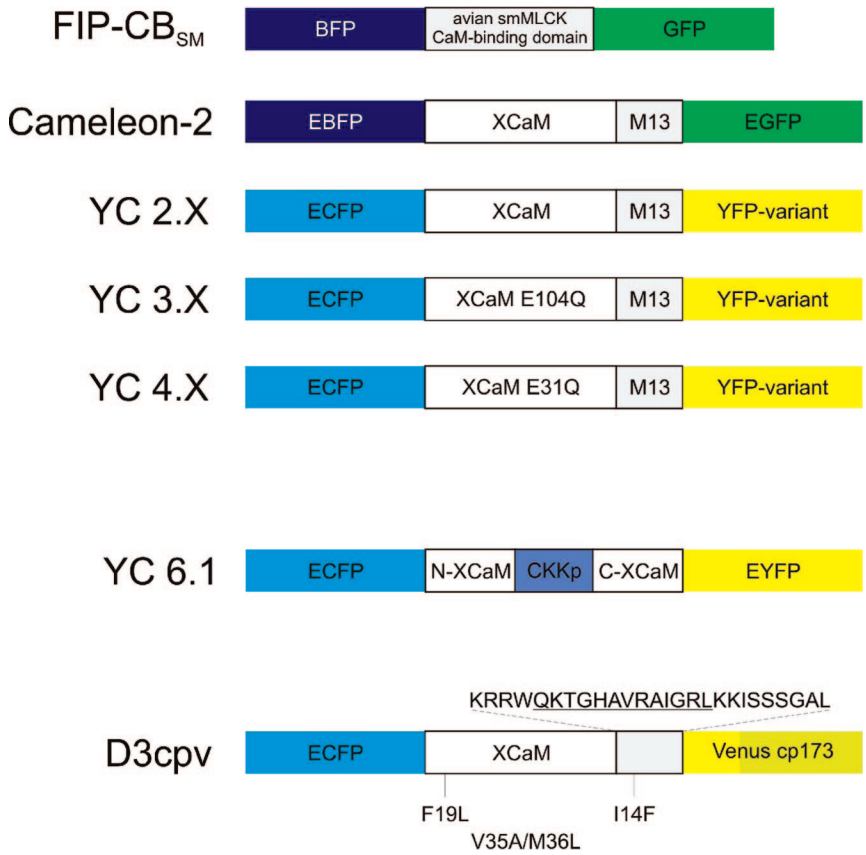

Figure 5. Calmodulin/FRET-based calcium indicators. Two prototypes can be distinguished. On one hand stands FIP-CB$_{SM}$, where the CaM-binding domain of the avian smooth muscle myosin light chain kinase (smMLCK) is sandwiched between BFP and GFP. The second building scheme is displayed by the Cameleons, where a fusion of XCaM and the M13 peptide of the muscle myosin light chain kinase is placed between EBFP and EGFP or ECFP and a YFP variant, respectively. Used YFP variants are YFP (X = 0), YFP-V68L/Q69K (X = 1), Citrine (X = 3), Venus (X = 12), and Venus cp173 (X = 6). One exception of this is found in Yellow Cameleon 6.1, where the CaM is split and the M13 peptide is replaced by the CaM-binding peptide of the CaM-dependent kinase kinase (Ckkp). The CaM-binding peptide in D3cpv consists of a hybrid of the CaM-binding domain of smMLCK (underlined) and skMLCK (skeletal muscle myosin light chain kinase). Note that the isoleucine at position 14 is replaced by a phenylalanine in D3cpv.

together between BFP and GFP (Figure 5).[49] These sensors were called "Cameleons". Upon binding, Ca^{2+}/calmodulin is thought to wrap around the neighboring M13 peptide, thereby initiating a conformational change of the chimeric protein and increasing energy transfer efficiency from BFP to GFP. The reasoning for including the calmodulin-binding peptide M13 was first of all to increase conformational change of the sensor complex. Second, the preferred intramolecular interaction of calmodulin with a neighboring binding peptide was thought to prevent the sensors from activating camodulin-dependent target proteins present within a cellular environment. The sensors could be calibrated and provided an accurate measure of free calcium concentrations. Moreover, instead of microinjection Cameleons were introduced into cells by DNA transfection, obliterating invasive labeling techniques and allowing the use of subcellular targeting sequences for sensor localization. Thus, the first live cell imaging of calcium dynamics in the nucleus and endoplasmic reticulum of HeLa cells was demonstrated with precisely localized Cameleons.[49] As it turned out, early variants of BFP were not suitable for working in live cells, as they were dim and bleached rapidly, even if codon-enhanced and folding optimized versions were used, as in Cameleon-2 (Figure 5).[49] Therefore the donor–acceptor pair was switched to Cyan Fluorescent Protein (CFP) and Yellow Fluorescent Protein (YFP) in Yellow Cameleon 2.0 (YC2.0) (Figure 5), which provided better signal-to-noise ratios and more stable imaging in live cells, at the cost of slightly higher spectral overlap of the CFP emission with the YFP emission band. Tuning calcium affinities was easily achieved by site-directed mutagenesis of chelating residues within EF-hand motifs of calmodulin.[49] While Cameleon-2 harboring wild-type calmodulin was reported to have a biphasic Ca^{2+} dependency with K_d's of 70 nM and 11 μM, substitution of glutamate 104 with glutamine within the third Ca^{2+}-binding loop of calmodulin resulted in the indicator Cameleon-3 with a lower affinity K_d of 4.4 μM, while the mutation E31Q shifted affinities to K_d's of 83 nM and 700 μM in Cameleon-4.[49] The latter two versions were especially suited to quantify higher amounts of free calcium as one would find in organelles such as the endoplasmic reticulum. Further engineering efforts to improve Cameleons were intended both to make the sensor less susceptible to perturbations by the cellular physiology and to improve signal strength of the indicators. Therefore many updated versions of Cameleons exist, with a nomenclature that unfortunately is not completely consistent. From YC2.0 on, the numbering indicated modifications of the calcium-sensing moiety, mainly changing affinity, with updates of the GFPs used as donors and acceptors given at one decimal place (but see YC2.12 and YC6.1).[50,51] While CFP fluorescence remained relatively stable down to approximately pH 6 and did not require immediate attention, one line of improvements consisted in replacing YFP as acceptor.[52] Having a pK_a of 7.0 it was maximally sensitive to small pH fluctuations in the cytosol, which can range from 6.8 to 7.3 under various conditions,

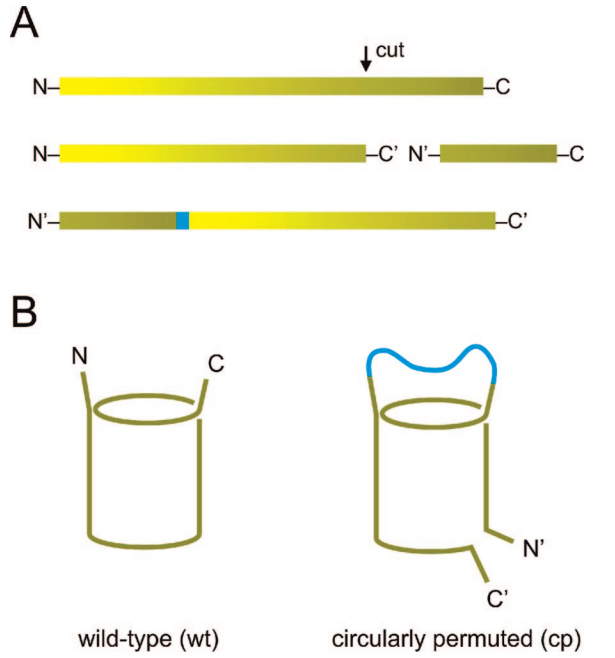

Figure 6. Circular permutation of GFPs. (A) Circularly permutated (cp) variants are obtained by opening of the wild-type protein sequence at an additional site. The resulting fragments are exchanged and combined by a short linker sequence (blue), which fuses the original N- and C-terminus. A number of permutations are possible in this way that result in functional chromophore formation. (B) Circularly permuted proteins are thought to display the same three-dimensional structures as their wild-type counterparts but have new N- and C-termini. The graph depicts a circularly permutated GFP variant with a presumed new N-terminus starting at amino acid 173 of Aequoria GFP (cp173).

thus generating pH-induced artifacts.[41,52,53] Another problem was quenching of YFP by halides, chloride being especially physiologically relevant in this respect.[40,42] As donor and acceptor fluorophores should be environmentally insensitive and only modulated by the FRET process, other variants of YFP were needed. A first remedy was replacing YFP with YFP-V68L/Q69K, which had a pK_a of 6.1.[53] Therefore Yellow Cameleon 2.1 incorporating YFP-V68L/Q69K as acceptor was less pH-sensitive at physiological ranges, at the cost of slightly reduced folding efficiency at 37 °C.[53] An even better solution turned out to be the YFP variant Citrine.[54] The mutation Q69 M within Citrine further shifted the pK_a to 5.7, which rendered it insensitive to pH changes in the cytosol. It folded well at 37 °C and was also insensitive to chloride concentrations, as the mutation Q69 M blocked an anion-binding cavity near the chromophore.[54] Subsequently another YFP variant termed Venus was shown to have similar environmental insensitivity, rendering Cameleons employing Citrine or Venus (YC 2.3/3.3/4.3 or YC2.12) (Figure 5) superior to and less artifact-prone than older versions.[50,54] To increase signal strength of Cameleons, one study replaced the M13 peptide with another calmodulin-binding peptide from calmodulin-dependent kinase kinase (CKKp) leading to YC6.1, which showed about twice as large signals in HeLa cells stimulated with histamine compared to the older YC2.1.[51] The most significant boosts in signal strength came from work involving circular permutation of GFP.[55–57] Circular permutations of GFP result in variants in which amino and carboxy portions of the proteins are interchanged (Figure 6). The original N- and C-termini are linked via a short peptide sequence so that new N- and C-termini become available for fusing the fluorophore to the calcium-binding domain (Figure 6). Therefore circularly permutated donor and acceptor proteins will have new angles of orientation to each other when fused to the sensor domain in this way. The manipulation of orientation and probably also distance would be expected to affect FRET efficiency from donor to acceptor fluorophore. Indeed, incorporating a circularly permuted form of Venus (Venus cp173) as an acceptor into YC2.60/3.60 resulted in a more than 5-fold maximal change in emission ratio *in vitro* from zero calcium to calcium saturation.[57] All the Cameleons so far use the calcium-dependent interaction of calmodulin with one of its target peptides to initiate a conformational change. The use of calmodulin within biosensors soon raised a number of concerns (see also next sections). One complication simply arises from large amounts of endogenous calmodulin being present in many cells, which may interact with the sensors binding peptide and thus inactivate the sensor. The "Design" series of calmodulin-based calcium sensors (Figure 5) therefore contained reengineered binding interfaces of calmodulin and its binding peptide, making these sensors insensitive to large excesses of endogenous calmodulin.[58,59] It provided a new series of improved Cameleons with calcium affinities ranging from 0.6 to 160 μM and large dynamic ranges from 3.8- to 5.3-fold.

3.2. FRET-Based Sensors Employing Troponin C (TnC)

While the efforts of Palmer and colleagues generated calmodulin-based biosensors with large ratio changes and resistance to perturbations by endogenous calmodulin, a number of other calmodulin-related problems may not have been fixed, for example the interactions with the numerous calmodulin-binding proteins (see also section 5 below).[59] A better solution therefore appeared to be the complete replacement of the highly regulated calmodulin with another calcium-binding protein that is not involved in signal transduction. Ideally such a protein could be a completely artificial design generated *de novo* on the drawing board. With such a solution not being close at hand at the moment, one would instead choose a specialized protein, possibly from a species that is phylogenetically not in close relationship with the organism and organ to be studied. A number of EF-hand-containing calcium-binding proteins exist in lower invertebrates, protozoa, and algae. For use in the mouse brain however, a number of other issues such as folding and protein function at 37 °C or codon usage are also worth considering.

Troponin C (TnC) from skeletal and cardiac muscle appears an acceptable compromise in this respect. It is a specialized calcium protein with no other known function than regulating muscle contraction. There are many variants of TnCs from invertebrate and vertebrate sources, offering alternatives and sequence diversity. The vertebrate variants of TnC appeared very suitable for expression and folding at 37 °C. TnC is not a free cytosolic protein, but part of the troponin complex where it functions in close association with troponin I and troponin T.[60] It is anchored to the complex via its C-terminal lobe through Ca^{2+}/Mg^{2+} binding. Therefore it came as a surprise that TnC-based sensors expressed well and without any signs of aggregation in living heterologous cells.[61,62] TnC-based Ca^{2+} sensors and Cameleons have a very similar architecture, both exploiting FRET between CFP and Citrine (and their variants), but differ in the Ca^{2+}-binding moiety and the lack of a binding peptide (Figure 7). The first sensors were based on chicken skeletal

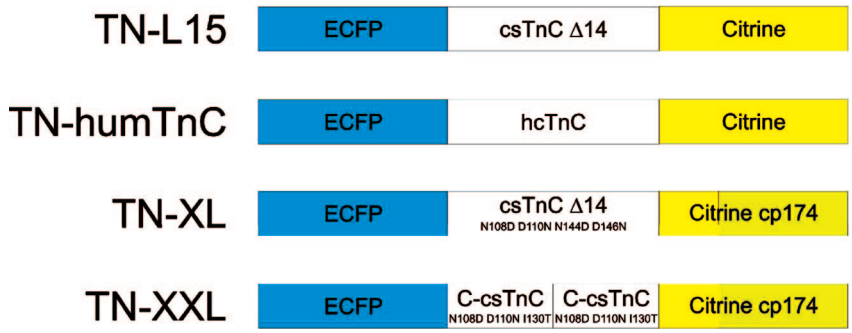

Figure 7. Troponin C/FRET-based calcium indicators. TN-L15 exploits a truncated version of chicken skeletal TnC as calcium-binding moiety. Human cardiac troponin C (hcTnC) constitutes the calcium-binding domain in TN-humTnC. Employing a circularly permuted variant of the Citrine and disrupting the Z-acid pairs in EF3 and EF4 led to TN-XL. The latest member of the troponin C-based family of calcium indicators is represented by TN-XXL. The C-terminal part of csTnC was doubled and sandwiched between the two GFP variants.

muscle TnC and human cardiac muscle TnC and were named TN-L15 and TN-humTnC, respectively.[61] These sensors provided high-affinity calcium binding (K_d's of 1.2 and 0.47 μM), but EF-hand mutagenesis also yielded low-affinity variants to quantify larger calcium transients. For example, the D107A mutation shifted the K_d of TN-L15 to 29 μM.[61] Further work yielded CerTN-L15 (K_d 1.2 μM), which was optimized for brightness when expressed in tissues by the substitution of CFP with its brighter variant Cerulean.[63,64] The N- and C-terminal lobes of vertebrate TnC's display differing calcium-binding properties. While the N-terminus binds calcium specifically with medium affinity, the C-terminus binds calcium with high affinity and also binds magnesium competitively.[36,37] Magnesium binding to the C-terminal EF-hands of TnC elicits a conformational change in the protein detectable by FRET.[62] In the resting state these two sites are partially bound by magnesium, reducing the amount of FRET change that can be obtained by raising calcium in the cell. Moreover, Mg^{2+} dissociation from these sites is relatively slow (k_{off} 8 s^{-1}), resulting in a slow replacement of Mg^{2+} with Ca^{2+} once the free cellular calcium rises. To address these issues, Mank and colleagues engineered the C-terminal EF-hands of troponin C within the TN-L15 backbone.[62] By eliminating the Z-acid pairs of EF-hands III and IV, magnesium-induced FRET change within the indicator was completely abolished, at the cost of a slightly reduced calcium affinity (K_d 2.5 μM). Moreover, the dynamic range of the sensor could be increased in analogy to YC3.60 by incorporation of circularly permutated Citrine as acceptor protein. The biosensor named TN-XL (for X-large FRET change) exhibited a roughly 5-fold increase in signal strength upon changing Ca^{2+} concentration from zero to saturation.[62] Engineering of calcium- and magnesium-binding sites also endowed TN-XL with extremely favorable kinetic properties. Thus, when expressed in *Drosophila* motoneurons, TN-XL allowed the measurement of presynaptic Ca^{2+} signals with the fastest rise (430 ms) and decay (240 ms) times reported so far for Ca^{2+} biosensors. Taking into account its intermediate affinity and its relatively fast kinetic properties (for current GECI standards), TN-XL may prove useful for subcellular targeting to sites where higher and more rapidly fluctuating calcium levels are expected. An example of such targetings is the fusion of TN-XL to the cytoplasmic mouth of an N-type calcium channel to directly monitor calcium at the channel pore (BPS abstract: 08-A-1927-BPS). Another line of optimization of TnC-based calcium biosensors is aimed at obtaining higher signals in the low to medium range of free calcium concentrations (100–500 nM). This is especially important to detect small calcium rises due to subtle physiological activities or single action potential firing within neurons. Higher sensitivity was achieved by rearrangement of troponin C, that is, the doubling of the C-terminal lobe and complete removal of the low affinity N-terminal lobe within the biosensor construct (Figure 7). Combined with a series of point mutations within the C-terminus of TnC to enhance FRET changes and increase affinity, this rearrangement provided an almost 2.5-fold enhancement of FRET signals between zero and 1.4 μM free calcium compared to TN-L15 (Mank and Griesbeck, unpublished observations). Thus, this new indicator, named TN-XXL, will most likely make the previous high-affinity sensors TN-L15, CerTN-L15, and TN-humTnC obsolete. A titration of TN-XXL as an example of a FRET-based calcium biosensor is shown in Figure 8.

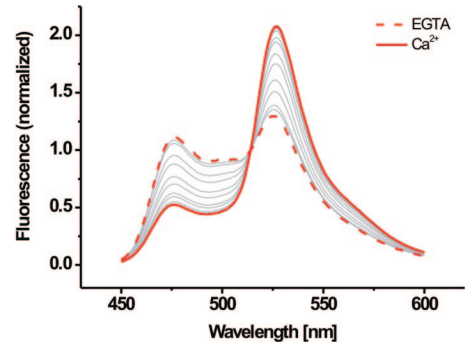

Figure 8. Calcium titration of TN-XXL. Shown are fluorescence emission spectra obtained at different calcium concentrations. The dashed red line reflects the emission spectrum seen in zero calcium/1 mM magnesium. The solid red line corresponds to 40 μM calcium/1 mM magnesium. Gray traces show intermediate spectra from various free calcium values between 65 nM calcium/1 mM magnesium and 30 μM calcium/1 mM magnesium. Note the decay of the CFP (475 nm) and the corresponding increase of the YFP (527 nm) due to FRET. Excitation was at 432 nm.

3.3. Single Fluorophore Sensors

The engineering of calcium biosensors based on a single XFP started with the surprising discovery by Baird et al. that the β-barrel of GFP tolerated the insertion of large protein fragments without destroying fluorescence, provided a suitable insertion site is found.[56]

Moreover, replacement of tyrosine 145 in YFP with the complete amino acid sequence of calmodulin resulted in a

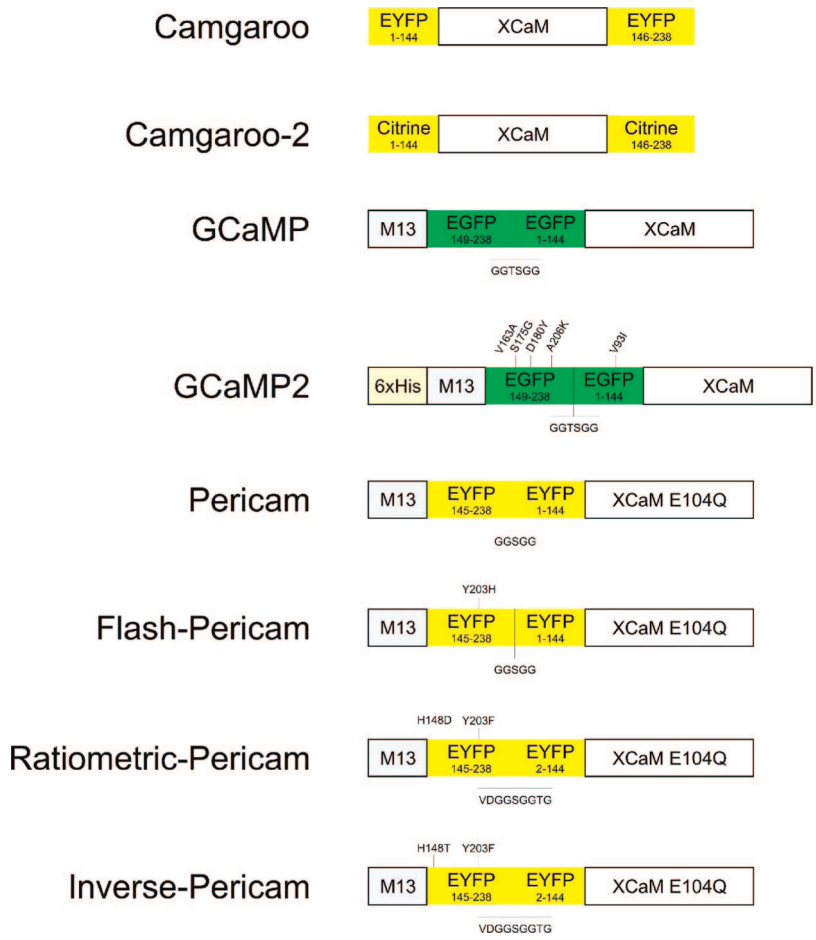

Figure 9. Selection of single fluorophore calcium indicators. These calcium sensors can be divided into three main classes, namely, Camgaroos, GCaMPs, and Pericams. The Camgaroos use YFP variants as chromophore in which *Xenopus* calmodulin is inserted. GCamP's make use of a circularly permuted EGFP with an N-terminal M13 peptide and a C-terminal attached CaM. The building scheme of Pericams is close to that of GCaMP's but instead they exploit YFP.

fusion protein whose fluorescence properties were modulated by the free calcium concentration. In this construct, named Camgaroo (Figure 9), calcium binding modified YFP fluorescence by promoting deprotonation of the chromophore at a constant pH. This was indicated by a shift of the absorbance spectrum from a predominant peak at 400 nm at zero calcium to a 490 nm absorbance peak at calcium saturation, which corresponded to the protonated form of YFP. Given that the protonated form of the chromophore absorbing maximally at 400 nm does not lead to fluorescence in YFP, the effect of calcium addition on the excitation and emission spectrum was a simple increase in magnitude, without any apparent spectral shifts. Accordingly, Camgaroo had different pH titration curves in the presence (pK_a 10.1) and absence of calcium *in vitro* (pK_a 8.9), qualifying it as a calcium-dependent pH sensor. This intrinsic pH sensitivity together with an unfavorable K_d (7 μM) and lack of visibility at basal calcium concentrations were clear disadvantages for using Camgaroo in live mammalian cells. An updated Camgaroo-2 (Figure 9) provided visibility of transfected cells under baseline conditions, but did not significantly improve the other parameters.[54] Moreover, its photophysical behavior appeared to be difficult to control.[65]

In "Pericams" the fluorophore backbone for the calcium biosensor was a circular permutation of YFP-V68L/Q69K because it promised a higher degree of sensitivity for manipulating its inner proton network by ligand-binding domains.[66] The permutation used Y145 as its new N-terminus fused to the M13 peptide and N144 as C-terminus fused to calmodulin E104Q (Figure 9). Manipulating the GFP network by point mutagenesis and a number of linker adjustments yielded three indicators with different response properties. Mutation Y203H generated "Flash-Pericam" (K_d 0.7 μM), a sensor whose excitation and emission amplitude increased about 8-fold with calcium. Introducing the mutation Y203F, a mutation known to render the nonfluorescent protonated 400 nm absorbance peak of YFP into an fluorescence-emitting species, generated "Ratiometric Pericam" (K_d 1.7 μM) (Figure 9), an indicator whose excitation wavelength changed with calcium. Combining Y203F with H148T resulted in "Inverse Pericam" (K_d 0.2 μM), a bright calcium biosensor whose fluorescence decreased upon calcium binding down to about 15% of the values at zero calcium. One possible advantage of such a protein may be that it is brightly fluorescent at resting state, making it easy to find cells expressing the sensor or to identify subcellular structures of interest. In contrast, "Flash Pericam" turned out to be almost invisible at resting states and also folding poorly at 37 °C.

The most popular of the single fluorophore sensors in recent years turned out to be G-CaMP and its updates.[67] Instead of using YFP cp145 as fluorescence backbone, G-CaMP employs EGFP cp149-144, thereby deleting amino acid residues 145 to 148 of EGFP. As calcium-binding moiety the authors stuck to calmodulin and its interaction partner M13, which were fused to the C- and N-terminus of

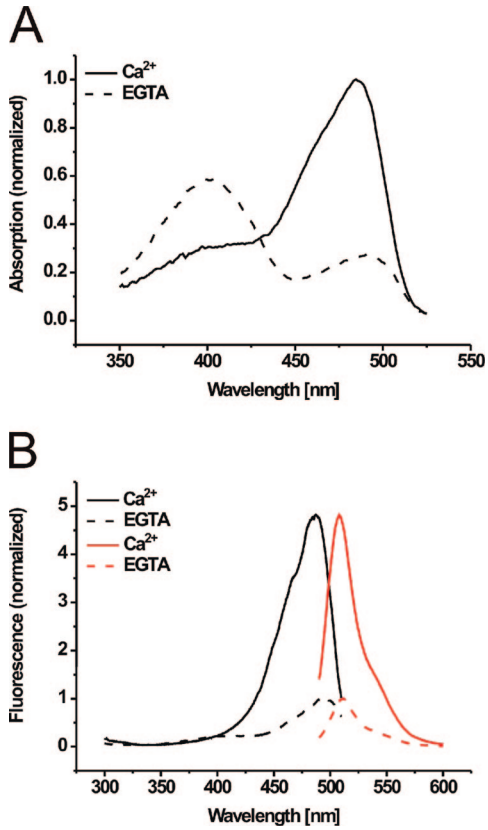

Figure 10. Absorption and fluorescence spectra of GCaMP2 as an example of a single fluorophore biosensor. (A) Normalized absorption spectra of GCaMP2 in calcium-free (EGTA, dashed line) and calcium-saturated (Ca^{2+}, solid line) state. (B) Normalized (to peak values obtained at zero calcium) fluorescence excitation (black lines) and fluorescence emission (red lines) spectra of GCaMP2 in both states. Data kindly provided by J. Nakai.

EGFP cp149-144, respectively. In this configuration calmodulin and M13 would be neighbors in the fully folded protein and be able to interact with each other in a calcium-dependent manner. As it turned out, the linker sequences used to fuse M13 and calmodulin to the cpEGFP moiety turned out to be critical for tuning response properties of G-CaMP. Therefore many different combinations were tried and tested to obtain a satisfying probe. In the cuvette G-CaMP showed an approximately 4.5-fold increase in fluorescence with calcium and an initially reported *in vitro* K_d of 235 nM. Calcium addition changed the absorbance spectrum of G-CaMP by decreasing the 400 nm peak and increasing the 490 nm peak, suggesting ionization of the chromophore, similar to other single fluorophore sensors (Figure 10).[67] Therefore, also G-CaMP possesses intrinsic pH sensitivity. Other disadvantages of the first version were dim fluorescence at resting states, poor folding, and slow maturation at 37 °C as well as nonlinear bleaching.[67,68] To address these issues, the common folding mutations V163A and S175G were incorporated into the cpEGFP moiety of G-CaMP, resulting in G-CaMP1.6 (K_d 146 nM), a brighter sensor variant with improved expression properties at 37 °C (Figure 9).[69] The latest update on the road to a bright and well-folding sensor is G-CaMP2, which was obtained by PCR-mediated mutagenesis of G-CaMP1.6 and screening of *E. coli* bacterial colonies for bright fluorescence at 37 °C.[70] Two mutations, D180Y and V93I, within the cpEGFP moiety were identified as critical for enhanced thermal stability of G-CaMP2 at 37 °C. As a result, G-CaMP2 was about 6-fold brighter than G-CaMP1.6, while retaining the relative 5-fold fractional fluorescence change of its ancestors. Interestingly, and a lesson for any further screening strategies to improve biosensor performance, the polyhistidine tag that was fused to any bacterial clone of the mutated library to facilitate subsequent purification turned out to be just as crucial for fluorescence at 37 °C. Removal of the tag resulted in loss of fluorescence at 37 °C. Therefore the polyhistidine tag was retained within the sensor in any expressions in nonbacterial cells.

Finally, another group used the principle architecture of Pericams as platform for the evolution of a biosensor with larger fractional change.[71] The best mutant, Case16 (K_d 1 μM), was reported to have a 16-fold fractional fluorescence increase with calcium. More data in living cells and more appropriate physiological context will however be necessary to fully evaluate the new probe.

All single fluorophore sensors mentioned so far achieve a calcium-dependent fluorescence change by a switch in the protonation status of the chromophore, a strategy that brings along an inherent pH sensitivity of the sensors. One may argue that this is a problem restricted to a limited number of cell types where larger cytosolic pH fluctuations occur. However, often calcium changes and pH fluctuations are closely intertwined in live cells and intracellular pH fluctuations are induced by many forms of neuronal activity, so that in the worst case scenario sensors will report a mixture of calcium and pH changes.[72,73] Are there any better ways to couple calcium binding to fluorescence changes? In particular it would appear desirable to manipulate XFP fluorescence by twisting and distorting the chromophore vicinity through conformational change that does not affect chromophore ionization. There appears to be one example of single fluorophore calcium biosensors that employs such a strategy for achieving a fractional fluorescence change. In "Inverse Pericams" high calcium leads to a slight blue shift of the 503 nm absorbance peak to 490 nm, without affecting the small peak at 400 nm, suggesting that changes in fluorophore intensity have been brought about predominantly by a structural change around the chromophore.[66]

4. In Vitro Kinetics

Some calcium imaging applications require sensors with fast binding kinetics to resolve rapid calcium fluctuations, for example within microdomains and sparks near channels and release sites. Also improved temporal resolution of action potentials within bursts depends on rapid kinetic indicator properties. Although it is difficult to compare kinetics measurements because of differences in temperature and ionic strength of buffer solutions, a few numbers may illustrate the current discrepancy between synthetic dyes and GECIs in that respect: While many synthetic dyes (including the high affinity indicators Fura-2, Fluo-3, and Calcium-Green-1) have K_{on} values of 10^8-10^9 M^{-1} s^{-1}, the value for Cameleon-1/E104Q ($K_d = 4.4$ μM) was reported to be 2.4×10^6 M^{-1} s^{-1}, which is a difference of approximately 2 orders of magnitude.[49,74] K_{off} values were from 100 to 370 s^{-1} (Calcium-Green-1, Fura-2, Fluo-3) versus 12.9 s^{-1} for Cameleon-1/E104Q.[49,74] Binding studies have been performed on the N-terminal lobes of TnC and calmodulin measuring fluorescence enhancement of tryptophans engineered in the vicinity of the calcium-binding sites.[75,76] Tryptophan quantum yields at 340 nm emission are increased approximately 3-fold in these mutants upon calcium binding

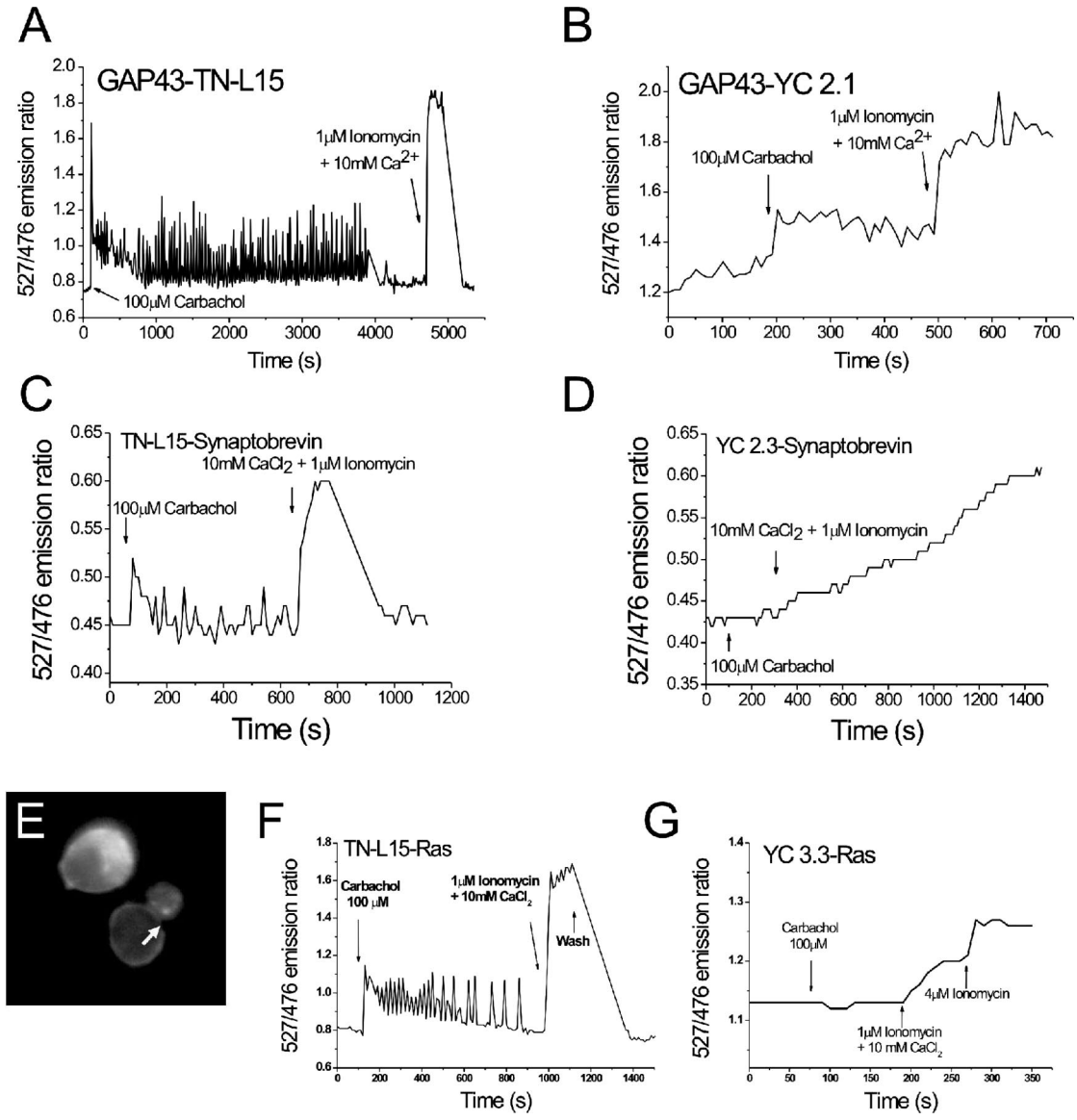

Figure 11. Comparison of troponin C-based and calmodulin-based FRET calcium sensors targeted to the plasma membrane of HEK293 cells. Constructs were made in an identical manner and differed only in their calcium-binding moiety. A and B compare constructs targeted to the membrane using the N-terminal GAP-43 targeting sequence. A shows an imaging trace of GAP43-TN-L15. Note that the construct was fully functional. B shows an imaging trace using the analogous GAP43-YC2.1. No oscillations were detectable, and only a modest response to ionomycin/10 mM $CaCl_2$ was seen. Ionomycin is an ionophore typically used to clamp cellular free calcium for *in situ* calibrations where a minimal indicator emission ratio R_{min} at zero calcium and a maximal emission ratio R_{max} at calcium saturation are used in the equation $[Ca^{2+}] = K_d[(R - R_{min})/(R_{max} - R)]^{(1/n)}$.[104] C and D compare membrane targetings by fusion of indicators to the C-terminus of synaptobrevin. TN-L15-synaptobrevin (C) retained calcium sensitivity in response to stimulation, although a limited dynamic range could be seen with this construct. YC2.3-synaptobrevin (D) had totally lost responsiveness to carbachol stimulation, although again a small, sluggish increase in ratio could be detected using ionomycin/10 mM $CaCl_2$. (E) Monochrome picture of the 293 cell whose race is shown in F. The arrow points at the cell that was imaged. F and G compare membrane targeting using the C-terminal targeting sequence of c-Ha-Ras. TN-L15Ras (F) was fully functional under these conditions and had comparable properties to the indicator when localized in the cytosol. (G) Imaging trace using YC3.3Ras under identical conditions. Reproduced with permission from ref 61. Copyright 2004 by the American Society for Biochemistry and Molecular Biology, ASBMB.

and present a more direct measure of binding. The data suggest that the inititial binding of calcium to EF-hands may not be more than 1 order of magnitude slower than binding to synthetic dyes.[75,76] Other studies determined diffusion-limited binding of calcium to the N-terminus of chicken skeletal and cardiac muscle troponin C with K_{on} of 10^8 M^{-1} s^{-1} and K_{off} of 500–800 s^{-1}, with off-rates at the high-affinity C-terminal lobe being 1 to 2 orders of magnitude slower.[77,78] There are indications that conformational change might be considerably slower than calcium binding/dissociation in some instances.[79] A recent study on calcium-induced conformational switching in calmodulin however reported very fast structural transitions with time constants of 490 μs and 20 ms for the C- and N-terminal lobe, respectively.[80] Temporal delays may certainly be caused by the coupling mechanisms that link calcium binding to EF-hands to optical read-out using fluorescent proteins. More insights into the biophysics of these mechanisms and structural information would certainly be useful. Could it be that the bulkiness of GFP or some so far unappreciated solvent interactions slow down the response of FRET biosensors? More recent GECIs such as TN-XL show faster fluorescence transition kinetics caused by increased K_{off}, however at the cost of losing affinity, as K_d is defined by K_{off}/K_{on}, and K_{on} was un-

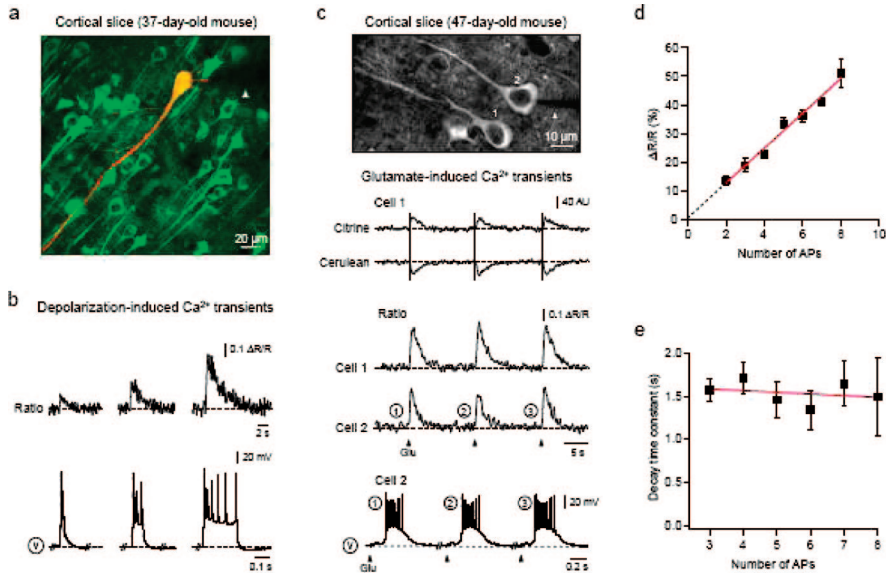

Figure 12. Transgenic expression of TN-L15 in the mouse brain using the Thy 1 promoter. (A) Merged image of layer 2/3 neurons in a cortical slice. TN-L15 labeling is shown in green; a pyramidal neuron patched with an internal saline containing 100 μM Alexa Fluor 594 is shown in yellow. Here and in C the shadow of the patch pipet is marked with an arrowhead. (B) Relative changes in the Citrine/Cerulean ratio and corresponding membrane depolarizations (lower; accompanied by 2, 4, and 7 APs, respectively) caused by three current injections (35, 100, and 300 ms long). (C) Upper: microphotograph of two layer 2/3 cortical neurons. Cell 1 is intact, whereas cell 2 is patched. Middle: original traces showing changes in fluorescence of donor and acceptor proteins in response to a 100 ms long iontophoretic glutamate application (cell 1) and corresponding ratio changes (cells 1 and 2). Lower: underlying bursts of action potentials recorded simultaneously from cell 2. Note similarity of ratio changes in the intact (cell 1) and patched (cell 2) cell. (D and E) Dependence of the amplitude of Citrine/Cerulean ratio of the cell shown in A to increasing numbers of action potentials and the decay time constant of the ratio changes on the number of underlying APs. Red lines are linear least-squares fits to the respective sets of data. Reproduced from ref 64.

changed.[62] Within the general relationship $K_d = K_{off}/K_{on}$ there may often be a tradeoff situation in which only one parameter of a GECI can easily be optimized at a time. Thus, the main advantage of synthetic calcium indicators is that they combine high calcium sensitivity with relatively rapid association and dissociation rates. To approximate the performance of synthetic dyes, both GECI K_{on} and K_{off} will have to be engineered, thus preserving affinity. In addition, the coupling mechanisms leading to changes in GFP fluorescence may need to be optimized. As a complicating factor, amino acid changes designed to affect kinetics may also have effects on the overall extent of conformational change and/or signal strength of a given indicator. Therefore, it appears that a sensor optimization strategy will have to operate in a multiparameter space, taking into account many variables simultaneously.

5. In Vitro versus in Vivo Performance

The titration and characterization of a fluorescent calcium indicator under controlled conditions *in vitro* is done in the hope that the measured indicator properties are maintained *in vivo* to accurately reflect fluctuations in free calcium inside living cells. However, already the experiences with synthetic calcium dyes teach us that the transition from an *in vitro* buffer solution to a cell's cytosol with a different environment of proteins and other biomolecules and slight differences in viscosity and concentrations of other ions can have detectable effects on the calcium-binding and fluorescence properties of an indicator.[81–83] The same is true for genetically encoded calcium indicators. Moreover, in the case of a protein-composed biosensor, the biological functions and interactions of the protein domains used to construct the biosensor have to be taken into consideration. As a biosensor needs to be expressed to a level of sufficient detectability, the protein will be present in the cell for an extended period of time before measurements start. In the case of transgenic expression, that may even be the whole lifetime of the animal, with ample time and opportunity for mutual interactions between the biosensor domains and cellular components. The GFPs derived from the jellyfish *Aequoria* appear in general biologically inert after expression in heterologous cells. Apart from sporadic reports of GFP-induced toxicity, the overwhelming number of successful biological studies using *Aequoria* GFPs suggests that toxicity or biological activity is not a major concern. For the more recent XFPs derived from Anthozoans there are not yet as many years of experience to benefit from. The early versions of DsRed and related FPs were reported to be aggregating inside live cells and toxic in some instances, but new variants appear as well tolerated as the *Aequoria* GFP variants.[84,85] One possible concern on the GFP side may lie in incomplete folding or chromophore oxidation under *in vivo* conditions, which may result in an inactive fraction of biosensor inside cells. A major source of problems in live cells however turned out to be the use of calmodulin as the calcium-binding moiety within indicators. Calmodulin is a ubiquitous signal protein in cell metabolism and thus under stringent regulation involving a plethora of calmodulin-binding proteins that sequester it and modulate its calcium-binding properties.[39] As an example, the IQ-motif binding proteins neurogranin and PEP-19 are expressed in excitatory neurons of rodents at significant levels. They both interact with apo-calmodulin and Ca^{2+}/calmodulin. Both have been shown to regulate binding and dissociation at its C-terminal lobe.[86,87] To what extent do these many known and unknown interactions of binding proteins distort the function of biosensors employing wild-type calmodulin as sensor moiety? Calmodulin also activates numerous kinases and phosphatases, modulates ion channels,

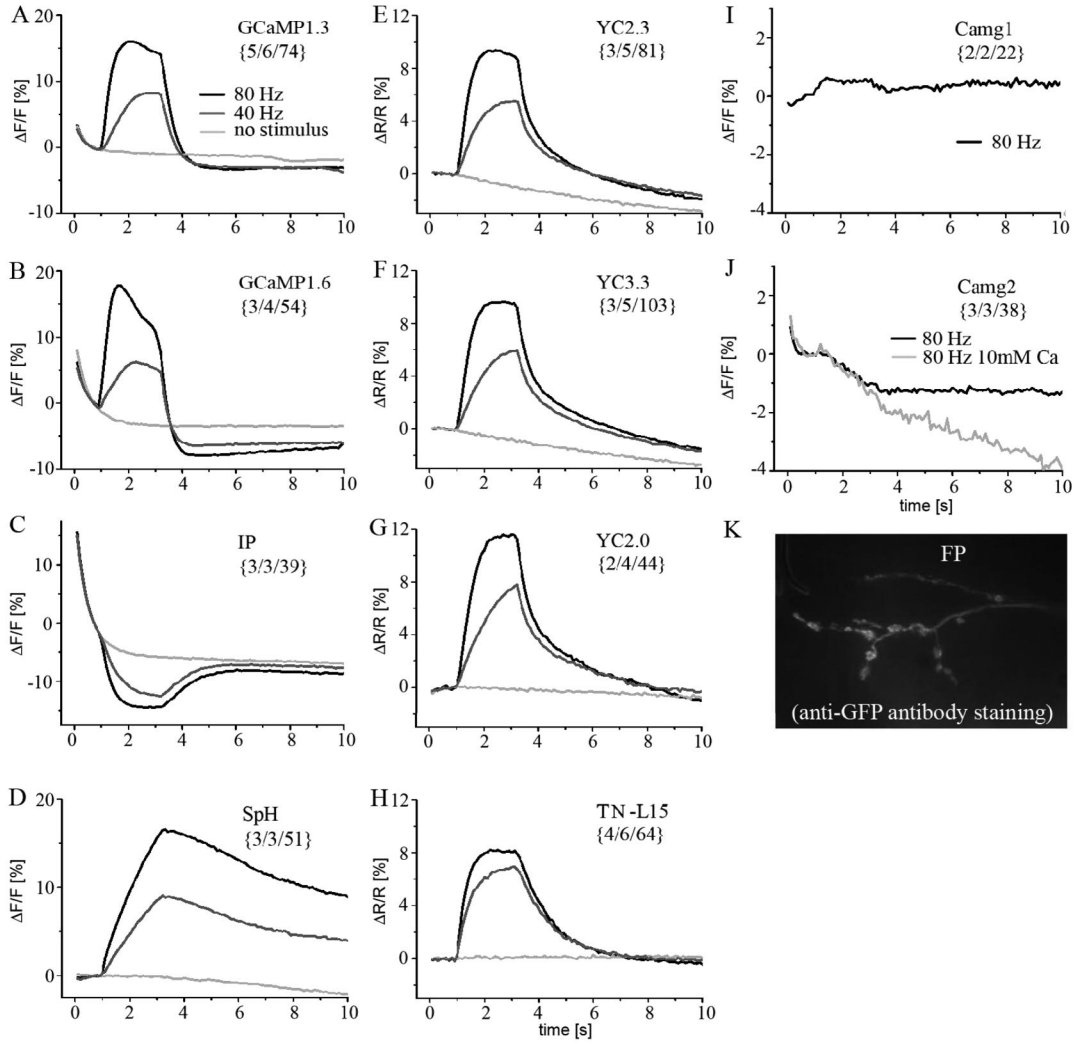

Figure 13. *In vivo* comparison of 10 different GECIs and synaptophluorin as reporters of neuronal activity at the *Drosophila* neuromuscular junction.[68,105] All indicators were tested under identical *in vivo* conditions. Nerve stimulation was performed at 0, 40, and 80 Hz (from $t = 1.2$ to 3.2 s), and presynaptic calcium changes were imaged using a CCD camera. (A−J) Traces for the individual biosensors. Standardized *in vivo* conditions such as these will be necessary for a solid evaluation of indicator performances. Reproduced with permission from ref 68. Copyright 2005 by the Society for Neuroscience.

and is itself extensively phosphorylated by multiple protein serine/threonine kinases and protein tyrosine kinases.[88–91] Accordingly, a number of researchers have encountered problems such as reduced or completely missing calcium sensitivity when using some of the wild-type calmodulin-based calcium sensors, predominantly when working with mammalian model systems. Results differed depending on the subcellular localization of the sensor and on the method of expression. For example, while acute transfection of Cameleons localized to the cytosol, nucleus, or endoplasmic reticulum of live HeLa or HEK 293 cells consistently yielded functional indicators, subcellular targetings to the plasma membrane of these cells frequently resulted in a loss of calcium sensitivity, although the localization and folding of the probe was correct (Figure 11).[49,61] Transgenic expression of Cameleons with cytosolic or membrane localization in mice also resulted in sensor inactivation in several instances. This included the expression of cytosolic YC3.0 using the CMV-actin promoter, the expression of cytosolic YC3.12 using a bidirectional TET promoter, and the expression of a membrane-targeted YC3.60 using another CMV-actin promoter construct.[57,92,93] In the first two examples a complete lack of calcium signals was reported, although the sensors appeared expressed and fluorescent.[85,86] One study noticed reduced diffusional mobility and punctuate fluorescence staining within cells of some transgenic lines.[93] In the latter case the discrepancy between an almost 600% ratio change *in vitro* and an approximately 2% relative acceptor channel fluorescence change in hippocampal slices of these mice after strong tetanic stimulation of the Schaffer collateral pathway is equally remarkable.[57] In contrast to these data transgenic expression of the TnC-based CerTN-L15 in the mouse brain resulted in functionality of the sensor (Figure 12).[64] Cameleons and TN-L15 are essentially identical in architecture and working principle and only differ in their calcium-binding moiety (Figures 4 and 7). Subcellular targetings to the plasma membrane are also functional when using a TnC-based sensor (Figures 9 and 11) or a sensor derived from the Design-Series with re-engineered CaM/M13 interface, suggesting that the high concentrations of endogenous calmodulin underneath the plasma membrane interfere with the proper function of the CaM/M13 module.[59,61] Results with single fluorophore sensors differ from those obtained with FRET sensors. It appears that their different architecture and working principle are less sensitive to interference by endogenous calmodulin or to sequestration due to calmodu-

Table 1. *In Vitro* Parameters of the Most Commonly Used GECIs[a]

	indicator	binding moiety	$\Delta F/F$, $\Delta R/R$	K_d	Hill coeff	kinetics	ref
single fluorophore	Camgaroo-1	wtCaM	600%	7.0 μM	1.6		56
indicators	Camgaroo-2	wtCaM	600%	5.3 μM	1.2		54
	F-Pericam	wtCaM (E104Q)/M13	700%	0.7 μM	0.7		66
	I-Pericam	wtCaM (E104Q)/M13	85%	0.2 μM	1.0	940 ms	66, 68
	R-Pericam	wtCaM (E104Q)/M13	900%	1.7 μM	1.1		66
	GCaMP(1.3)	wtCaM/M13	350%	0.24 μM	3.3	330 ms	67, 68
	GCaMP1.6	wtCaM/M13	400%	0.15 μM	3.8	260 ms	68, 69
	GCaMP2	wtCaM/M13	400%	0.15 μM	3.8		70
fret-based	YC2.0	wtCaM/M13				350 ms/3070 ms	49, 68
Indicators	YC2.1	wtCaM/M13		0.1 μM/4.3 μM	1.8/0.6		53
	YC3.1	wtCaM (E104Q)/M13		1.5 μM	1.1		53
	YC2.6	wtCaM/M13	560%	0.04 μM	2.4		57
	YC3.6	wtCaM (E104Q)/M13	560%	0.25 μM	1.7		57
	YC4.6	wtCaM(E31Q)/M13	360%	0.06 μM/14.4 μM	1.7/0.9		57
	D1	redesigned CaM		0.81 μM/60 μM			58
	D2cpv	redesigned CaM	430%	0.03 μM/3 μM			59
	D3cpv	redesigned CaM	410%	0.6 μM			59
	D4cpv	redesigned CaM	280%	64 μM			59
	TN-L15	TnC	140%	1.2 μM	1.0	1330 ms	61, 68
	TN-XL	TnC	400%	2.5 μM	1.7	240 ms	62, 68
	TN-XXL	TnC	230%	0.8 μM	1.5		

[a] Dissociation constants, signal strength, and Hill coefficients were extracted from the original publications as obtained from recombinant purified indicator proteins. Signal strength is depicted as $\Delta F/F_{max}$ or $\Delta R/R_{max}$ values in %. Kinetic values represent the decay time constant obtained from transgenically expressed indicators at the *Drosophila* larval neuromuscular junction after stimulation of the motorneuron at 40 Hz according to ref 68.

lin-binding proteins. Thus, transgenic expression of Pericams and G-CaMPs in the mouse resulted in functional sensors in skeletal muscle, in heart muscle, and in the brain.[70,93–96] It should be noted that interactions between sensor and host cell biochemistry may not work in only one direction. While many of the results described above document interference of cellular proteins with wild-type calmodulin-based sensor functionality, overexpression of the biosensor may be able to induce a phenotype that modifies the cell to be studied. Indeed, transgenic expression of G-CaMP2 in the heart of transgenic mice induces cardiomegaly, a phenotype resembling the overexpression of plain calmodulin under the same context.[70] Thus, the CaM/M13 module may not be as restricted to intramolecular interaction as previously thought, but instead allowing excessive activation of many calmodulin-dependent signaling pathways. While the phenotype of cardiomegaly is not easily missed, effects in other tissues such as the nervous system may be more subtle. Careful analysis should be performed to rule out that overexpression of such sensor leads to unphysiological modulation of calmodulin-dependent kinases and ion channels, which could set off the physiology and rules of plasticity of the neuron to be studied.

6. Detecting Neuronal Activity

GECIs have exquisite advantages for loading populations of neurons in intact animals. They can be targeted to subtypes of neurons or subcellular sites of interest, are noninvasive, allow chronic imaging over extended periods of time, and facilitate the labeling of long processes extending over distances of several hundred micrometers.[64] For these reasons it would be attractive to use them for the study of neuronal activity such as done with synthetic dyes. The ideal GECI reporter of neuronal activity would be insensitive to levels of resting calcium, but responding at high signal-to-noise levels to low-level activity such as small calcium rises due to firing of one or a few action potential. Fast kinetic fluorescence responses of such a reporter would help resolve incremental increases with numbers of action potentials and allow a better representation of activity patterns by the indicator fluorescence. Relationships between calcium and activity to fluorescence changes should at best be linear. A sensor would need to show relatively high affinity calcium binding and high fluorescence changes in the low calcium concentration range, as calcium rises due to one or a few action potentials are in the range of a few hundred nanomolar.[97–99] In this respect one certainly will have to find a tradeoff line between high-affinity binding properties and buffering potential during chronic expression of the biosensor within an animal. The first-generation GECIs analyzed so far were reporting reliably high frequency activity, but were relatively insensitive to low-frequency stimulation such as one or two action potentials (Figures 12 and 13).[64,68,100] Single action potentials could not be resolved in single trials, but only after averaging of a very large number of runs.[100] Frequency domain analysis indicated that GECIs such as first-generation G-CaMP responded too slowly to follow individual action potentials within a burst.[100] Presumably second-generation biosensors such as YC3.60, D3cpV, G-CaMP2, and TN-XXL will offer some improved response properties, but more efforts are needed. As some areas of the brain such as the mouse somatosensory cortex work in sparse coding mode with single action potentials fired every 20 s, single trial sensitivity is required.[101] Nonlinearity between neuronal activity, calcium dynamics, and GECI fluorescence responses has been reported and reflects the intrinsic calcium-binding properties of the used sensor domains.[100] New tools have been developed that help to understand relationships between GECI signals, calcium dynamics, and firing rates that will be useful for interpretation of signals.[102,103] It should be kept in mind that apart from calcium affinity and magnitude of fluorescence change the brightness of biosensor expression within tissue is another important factor for *in vivo* work, determining sensitivity and the signal-to-noise ratio of recordings. XFPs have good quantum yields, but the extinction coefficients of variants are lower than those of many fluorescent chemical compounds. Until brighter XFPs are available one may have to

compensate by reaching higher expression levels. In general strong expression allows better signal-to-noise ratios, albeit at the cost of further kinetic slowing of responses.[68] Are FRET sensors or single fluorophore sensors preferable as activity reporters? In general, single fluorophore sensors are superior in terms of signal-to-noise levels from a theoretical point of view, but FRET sensors currently offer more photostability, more pH-resistance, better labeling of neuronal structure *in vivo*, and the benefit of ratiometric imaging. In particular under *in vivo* conditions where one faces a high degree of movement, artifacts due to blood flow and breathing of the animal ratioing may help eliminate these sources of correlated noise that equally affect both emission channels.

7. Conclusions

The development of genetically encoded calcium indicators has made considerable progress within the first 10 years of existence of the field. We learnted more about principles of coupling calcium binding to fluorescence changes and about increasing the signal strength of the indicators further. We also learned more about conditions for expressing these sensors in transgenic animals and what the possible caveats and complications are in using them for that purpose. Although biosensor performance is still behind that of the best synthetic dyes, many applications in cell biology and physiology are already possible with the existing sensors. Furthermore, the theoretical limits for GECI performance appear not to have been reached yet with the actual designs. Improvements certainly come with the advent of brighter XFPs, as the question of how many photons can be retrieved from a sensor molecule is critical and limiting for imaging experiments. Brighter and possibly red-shifted XFPs will allow lower expression levels, and therefore improved kinetics, better visualization of structure, and better signal-to-noise levels within tissue. Another line of progress will arise from adapting the calcium-binding properties of the calcium-binding motifs better to the task of reporting neuronal activity in terms of affinity, linearity, conformational change, and kinetics. As structure–function relationships in these proteins are complicated, probably a combination of rational design and methods of directed molecular evolution will be necessary to yield the desired sensor modules. Ideally, the number of calcium-binding sites will also be reduced per indicator molecule while retaining large calcium-dependent fluorescence changes. It will have to be explored to what extent calcium-binding sites can be minimized and cooperativity abolished without sacrificing responsiveness in the physiological range. Evidently, the community will have to agree to common standards for evaluating and comparing the various sensors on the market under identical experimental conditions. An example for this may be the comprehensive analysis by Reiff and colleagues (Figure 13) of a large number of GECIs *in vivo* at the *Drosophila* neuromuscular junction.[68] Certainly a corresponding mammalian model system is needed. What should be a goal to reach with all these engineering efforts? As one of several points on the wish list we would like to propose that the detection of individual action potentials in single trials within the mouse cortex layer 3 *in vivo* would be a challenging and perhaps not unrealistic achievement.

8. Acknowledgments

We would like to thank Junichi Nakai for providing spectral data, Amy Palmer for comments on figures, and Alexander Borst and Dierk Reiff for comments on the manuscript. This work was supported by the Max-Planck-Society and DFG Priority Programme SP1172.

9. References

(1) Kleinfeld, D.; Griesbeck, O. *PLoS Biol.* **2005**, *3*, e355.
(2) Miesenbock, G.; Kevrekidis, I. G. *Annu. Rev. Neurosci.* **2005**, *28*, 533.
(3) Helmchen, F.; Denk, W. *Nat. Methods* **2005**, *2*, 932.
(4) Svoboda, K.; Yasuda, R. *Neuron* **2006**, *50*, 823.
(5) Callaway, E. M. *Trends Neurosci.* **2005**, *28*, 196.
(6) Shaner, N. C.; Steinbach, P. A.; Tsien, R. Y. *Nat. Methods* **2005**, *2*, 905.
(7) Verkhusha, V. V.; Lukyanov, K. A. *Nat. Biotechnol.* **2004**, *22*, 289.
(8) Chudakov, D. M.; Lukyanov, S.; Lukyanov, K. A. *Trends Biotechnol.* **2005**, *23*, 605.
(9) Wolff, M.; Wiedenmann, J.; Nienhaus, G. U.; Valler, M.; Heilker, R. *Drug Discovery Today* **2006**, *11*, 1054.
(10) Tsien, R. Y. *Annu. Rev. Biochem.* **1998**, *67*, 509.
(11) Remington, S. J. *Curr. Opin. Struct. Biol.* **2006**, *16*, 714.
(12) Kendall, J. M.; Badminton, M. N. *Trends Biotechnol.* **1998**, *16*, 216.
(13) Baubet, V.; Le Mouellic, H.; Campbell, A. K.; Lucas-Meunier, E.; Fossier, P.; Brulet, P. *Proc. Natl. Acad. Sci. U.S.A.* **2000**, *97*, 7260.
(14) Martin, J. R.; Rogers, K. L.; Chagneau, C.; Brulet, P. *PLoS ONE* **2007**, *2*, e275.
(15) Rogers, K. L.; Picaud, S.; Roncali, E.; Boisgard, R.; Colasante, C.; Stinnakre, J.; Tavitian, B.; Brulet, P. *PLoS ONE* **2007**, *2*, e974.
(16) Shimomura, O. *Cell Calcium* **1991**, *12*, 635.
(17) Jones, K.; Hibbert, F.; Keenan, M. *Trends Biotechnol.* **1999**, *17*, 477.
(18) Chiesa, A.; Rapizzi, E.; Tosello, V.; Pinton, P.; de Virgilio, M.; Fogarty, K. E.; Rizzuto, R. *Biochem. J.* **2001**, *355*, 1.
(19) Tsien, R. Y. *Annu. Rev. Neurosci.* **1989**, *12*, 227.
(20) Tsien, R. Y. *Am. J. Physiol.* **1992**, *263*, C723–C728.
(21) Garaschuk, O.; Milos, R. I.; Grienberger, C.; Marandi, N.; Adelsberger, H.; Konnerth, A. *Pflugers Arch.* **2006**, *453*, 385.
(22) Gobel, W.; Helmchen, F. *Physiology (Bethesda)* **2007**, *22*, 358.
(23) Tour, O.; Adams, S. R.; Kerr, R. A.; Meijer, R. M.; Sejnowski, T. J.; Tsien, R. W.; Tsien, R. Y. *Nat. Chem. Biol.* **2007**, *3*, 423.
(24) Siegel, M. S.; Isacoff, E. Y. *Neuron* **1997**, *19*, 735.
(25) Ataka, K.; Pieribone, V. A. *Biophys. J.* **2002**, *82*, 509.
(26) Dimitrov, D.; He, Y.; Mutoh, H.; Baker, B. J.; Cohen, L.; Akemann, W.; Knopfel, T. *PLoS ONE* **2007**, *2*, e440.
(27) Moldoveanu, T.; Jia, Z.; Davies, P. L. *J. Biol. Chem.* **2004**, *279*, 6106.
(28) Hilge, M.; Aelen, J.; Perrakis, A.; Vuister, G. W. *Ann. N.Y. Acad. Sci.* **2007**, *1099*, 7.
(29) Rizo, J.; Sudhof, T. C. *J. Biol. Chem.* **1998**, *273*, 15879.
(30) Verdaguer, N.; Corbalan-Garcia, S.; Ochoa, W. F.; Fita, I.; Gomez-Fernandez, J. C. *EMBO J.* **1999**, *18*, 6329.
(31) Shao, X.; Fernandez, I.; Sudhof, T. C.; Rizo, J. *Biochemistry* **1998**, *37*, 16106.
(32) Kretsinger, R. H.; Nockolds, C. E. *J. Biol. Chem.* **1973**, *248*, 3313.
(33) Gifford, J. L.; Walsh, M. P.; Vogel, H. J. *Biochem. J.* **2007**, *405*, 199.
(34) Grabarek, Z. *J. Mol. Biol.* **2006**, *359*, 509.
(35) Tikunova, S. B.; Black, D. J.; Johnson, J. D.; Davis, J. P. *Biochemistry* **2001**, *40*, 3348.
(36) Filatov, V. L.; Katrukha, A. G.; Bulargina, T. V.; Gusev, N. B. *Biochemistry (Moscow)* **1999**, *64*, 969.
(37) Potter, J. D.; Gergely, J. *Recent Adv. Stud. Cardiac. Struct. Metab.* **1975**, *5*, 235.
(38) Lewit-Bentley, A.; Rety, S. *Curr. Opin. Struct. Biol.* **2000**, *10*, 637.
(39) Jurado, L. A.; Chockalingam, P. S.; Jarrett, H. W. *Physiol. Rev.* **1999**, *79*, 661.
(40) Wachter, R. M.; Remington, S. J. *Curr. Biol.* **1999**, *9*, R628–R629.
(41) Llopis, J.; McCaffery, J. M.; Miyawaki, A.; Farquhar, M. G.; Tsien, R. Y. *Proc. Natl. Acad. Sci. U.S.A.* **1998**, *95*, 6803.
(42) Wachter, R. M.; Yarbrough, D.; Kallio, K.; Remington, S. J. *J. Mol. Biol.* **2000**, *301*, 157.
(43) Jayaraman, S.; Haggie, P.; Wachter, R. M.; Remington, S. J.; Verkman, A. S. *J. Biol. Chem.* **2000**, *275*, 6047.
(44) Kuner, T.; Augustine, G. J. *Neuron* **2000**, *27*, 447.
(45) Jares-Erijman, E. A.; Jovin, T. M. *Nat. Biotechnol.* **2003**, *21*, 1387.
(46) Förster, T. *Ann. Phys.* **1948**, *437*, 55.
(47) Heim, R.; Tsien, R. Y. *Curr. Biol.* **1996**, *6*, 178.

(48) Romoser, V. A.; Hinkle, P. M.; Persechini, A. *J. Biol. Chem.* **1997**, *272*, 13270.
(49) Miyawaki, A.; Llopis, J.; Heim, R.; McCaffery, J. M.; Adams, J. A.; Ikura, M.; Tsien, R. Y. *Nature* **1997**, *388*, 882.
(50) Nagai, T.; Ibata, K.; Park, E. S.; Kubota, M.; Mikoshiba, K.; Miyawaki, A. *Nat. Biotechnol.* **2002**, *20*, 87.
(51) Truong, K.; Sawano, A.; Mizuno, H.; Hama, H.; Tong, K. I.; Mal, T. K.; Miyawaki, A.; Ikura, M. *Nat. Struct. Biol.* **2001**, *8*, 1069.
(52) Miyawaki, A.; Tsien, R. Y. *Methods Enzymol.* **2000**, *327*, 472.
(53) Miyawaki, A.; Griesbeck, O.; Heim, R.; Tsien, R. Y. *Proc. Natl. Acad. Sci. U.S.A.* **1999**, *96*, 2135.
(54) Griesbeck, O.; Baird, G. S.; Campbell, R. E.; Zacharias, D. A.; Tsien, R. Y. *J. Biol. Chem.* **2001**, *276*, 29188.
(55) Topell, S.; Hennecke, J.; Glockshuber, R. *FEBS Lett.* **1999**, *457*, 283.
(56) Baird, G. S.; Zacharias, D. A.; Tsien, R. Y. *Proc. Natl. Acad. Sci. U.S.A.* **1999**, *96*, 11241.
(57) Nagai, T.; Yamada, S.; Tominaga, T.; Ichikawa, M.; Miyawaki, A. *Proc. Natl. Acad. Sci. U.S.A.* **2004**, *101*, 10554.
(58) Palmer, A. E.; Jin, C.; Reed, J. C.; Tsien, R. Y. *Proc. Natl. Acad. Sci. U.S.A.* **2004**, *101*, 17404.
(59) Palmer, A. E.; Giacomello, M.; Kortemme, T.; Hires, S. A.; Lev-Ram, V.; Baker, D.; Tsien, R. Y. *Chem. Biol.* **2006**, *13*, 521.
(60) Gordon, A. M.; Homsher, E.; Regnier, M. *Physiol. Rev.* **2000**, *80*, 853.
(61) Heim, N.; Griesbeck, O. *J. Biol. Chem.* **2004**, *279*, 14280.
(62) Mank, M.; Reiff, D. F.; Heim, N.; Friedrich, M. W.; Borst, A.; Griesbeck, O. *Biophys. J.* **2006**, *90*, 1790.
(63) Rizzo, M. A.; Springer, G. H.; Granada, B.; Piston, D. W. *Nat. Biotechnol.* **2004**, *22*, 445.
(64) Heim, N.; Garaschuk, O.; Friedrich, M. W.; Mank, M.; Milos, R. I.; Kovalchuk, Y.; Konnerth, A.; Griesbeck, O. *Nat. Methods* **2007**, *4*, 127.
(65) Filippin, L.; Magalhaes, P. J.; Di Benedetto, G.; Colella, M.; Pozzan, T. *J. Biol. Chem.* **2003**, *278*, 39224.
(66) Nagai, T.; Sawano, A.; Park, E. S.; Miyawaki, A. *Proc. Natl. Acad. Sci. U.S.A.* **2001**, *98*, 3197.
(67) Nakai, J.; Ohkura, M.; Imoto, K. *Nat. Biotechnol.* **2001**, *19*, 137.
(68) Reiff, D. F.; Ihring, A.; Guerrero, G.; Isacoff, E. Y.; Joesch, M.; Nakai, J.; Borst, A. *J. Neurosci.* **2005**, *25*, 4766.
(69) Ohkura, M.; Matsuzaki, M.; Kasai, H.; Imoto, K.; Nakai, J. *Anal. Chem.* **2005**, *77*, 5861.
(70) Tallini, Y. N.; Ohkura, M.; Choi, B. R.; Ji, G.; Imoto, K.; Doran, R.; Lee, J.; Plan, P.; Wilson, J.; Xin, H. B.; Sanbe, A.; Gulick, J.; Mathai, J.; Robbins, J.; Salama, G.; Nakai, J.; Kotlikoff, M. I. *Proc. Natl. Acad. Sci. U.S.A.* **2006**, *103*, 4753.
(71) Souslova, E. A.; Belousov, V. V.; Lock, J. G.; Stromblad, S.; Kasparov, S.; Bolshakov, A. P.; Pinelis, V. G.; Labas, Y. A.; Lukyanov, S.; Mayr, L. M.; Chudakov, D. M. *BMC Biotechnol.* **2007**, *7*, 37.
(72) Chesler, M.; Kaila, K. *Trends Neurosci.* **1992**, *15*, 396.
(73) Yao, H.; Haddad, G. G. *Cell Calcium* **2004**, *36*, 247.
(74) Naraghi, M. *Cell Calcium* **1997**, *22*, 255.
(75) Black, D. J.; Tikunova, S. B.; Johnson, J. D.; Davis, J. P. *Biochemistry* **2000**, *39*, 13831.
(76) Tikunova, S. B.; Rall, J. A.; Davis, J. P. *Biochemistry* **2002**, *41*, 6697.
(77) Johnson, J. D.; Nakkula, R. J.; Vasulka, C.; Smillie, L. B. *J. Biol. Chem.* **1994**, *269*, 8919.
(78) Li, M. X.; Saude, E. J.; Wang, X.; Pearlstone, J. R.; Smillie, L. B.; Sykes, B. D. *Eur. Biophys. J.* **2002**, *31*, 245.
(79) Hazard, A. L.; Kohout, S. C.; Stricker, N. L.; Putkey, J. A.; Falke, J. J. *Protein Sci.* **1998**, *7*, 2451.
(80) Park, H. Y.; Kim, S. A.; Korlach, J.; Rhoades, E.; Kwok, L. W.; Zipfel, W. R.; Waxham, M. N.; Webb, W. W.; Pollack, L. *Proc. Natl. Acad. Sci. U.S.A.* **2008**, *105*, 542.
(81) Snitsarev, V. A.; McNulty, T. J.; Taylor, C. W. *Biophys. J.* **1996**, *71*, 1048.
(82) Busa, W. B. *Cell Calcium* **1992**, *13*, 313.
(83) Tank, D. W.; Regehr, W. G.; Delaney, K. R. *J. Neurosci.* **1995**, *15*, 7940.
(84) Hirrlinger, P. G.; Scheller, A.; Braun, C.; Quintela-Schneider, M.; Fuss, B.; Hirrlinger, J.; Kirchhoff, F. *Mol. Cell Neurosci.* **2005**, *30*, 291.
(85) Livet, J.; Weissman, T. A.; Kang, H.; Draft, R. W.; Lu, J.; Bennis, R. A.; Sanes, J. R.; Lichtman, J. W. *Nature* **2007**, *450*, 56.
(86) Kubota, Y.; Putkey, J. A.; Waxham, M. N. *Biophys. J.* **2007**, *93*, 3848.
(87) Kubota, Y.; Putkey, J. A.; Shouval, H. Z.; Waxham, M. N. *J. Neurophysiol.* **2008**, *99*, 264.
(88) Hoeflich, K. P.; Ikura, M. *Cell* **2002**, *108*, 739.
(89) Saimi, Y.; Kung, C. *Annu. Rev. Physiol.* **2002**, *64*, 289.
(90) Mori, M. X.; Erickson, M. G.; Yue, D. T. *Science* **2004**, *304*, 432.
(91) Benaim, G.; Villalobo, A. *Eur. J. Biochem.* **2002**, *269*, 3619.
(92) Tsai, P. S.; Friedman, B.; Ifarraguerri, A. I.; Thompson, B. D.; Lev-Ram, V.; Schaffer, C. B.; Xiong, Q.; Tsien, R. Y.; Squier, J. A.; Kleinfeld, D. *Neuron* **2003**, *39*, 27.
(93) Hasan, M. T.; Friedrich, R. W.; Euler, T.; Larkum, M. E.; Giese, G.; Both, M.; Duebel, J.; Waters, J.; Bujard, H.; Griesbeck, O.; Tsien, R. Y.; Nagai, T.; Miyawaki, A.; Denk, W. *PLoS Biol.* **2004**, *2*, e163.
(94) Ji, G.; Feldman, M. E.; Deng, K. Y.; Greene, K. S.; Wilson, J.; Lee, J. C.; Johnston, R. C.; Rishniw, M.; Tallini, Y.; Zhang, J.; Wier, W. G.; Blaustein, M. P.; Xin, H. B.; Nakai, J.; Kotlikoff, M. I. *J. Biol. Chem.* **2004**, *279*, 21461.
(95) Diez-Garcia, J.; Akemann, W.; Knopfel, T. *Neuroimage* **2007**, *34*, 859.
(96) Chaigneau, E.; Tiret, P.; Lecoq, J.; Ducros, M.; Knopfel, T.; Charpak, S. *J. Neurosci.* **2007**, *27*, 6452.
(97) Borst, J. G.; Sakmann, B. *J. Physiol.* **1998**, *506* (1), 143.
(98) Helmchen, F.; Borst, J. G.; Sakmann, B. *Biophys. J.* **1997**, *72*, 1458.
(99) Markram, H.; Helm, P. J.; Sakmann, B. *J. Physiol.* **1995**, *485* (1), 1.
(100) Pologruto, T. A.; Yasuda, R.; Svoboda, K. *J. Neurosci.* **2004**, *24*, 9572.
(101) Kerr, J. N.; Greenberg, D.; Helmchen, F. *Proc. Natl. Acad. Sci. U.S.A.* **2005**, *102*, 14063.
(102) Borst, A.; Abarbanel, H. D. *Theor. Biol. Med. Model* **2007**, *4*, 7.
(103) Tay, L. H.; Griesbeck, O.; Yue, D. T. *Biophys. J.* **2007**, *93*, 4031.
(104) Adams, S. R.; Bacskai, B. J.; Taylor S. S.; Tsien, R. Y. *Fluorescent Probes for Biological Activity of Living Cells−A Practical Guide*; Academic: New York, 1993; p *133*.
(105) Miesenbock, G.; De Angelis, D. A.; Rothman, J. E. *Nature* **1998**, *394*, 192.

CR078213V